NASA TECHNICAL NOTE

NASA TN D-5685

NASA TN D-5685

DYNAMIC BEHAVIOR OF AIR LUBRICATED PIVOTED-PAD JOURNAL BEARING - ROTOR SYSTEM

I - Effects of Mount Stiffness and Damping

by Zolton N. Nemeth and William J. Anderson

Lewis Research Center
Cleveland, Ohio

NATIONAL AERONAUTICS AND SPACE ADMINISTRATION • WASHINGTON, D. C. • FEBRUARY 1970

1. Report No. NASA TN D-5685	2. Government Accession No.	3. Recipient's Catalog No.
4. Title and Subtitle DYNAMIC BEHAVIOR OF AIR LUBRICATED PIVOTED-PAD JOURNAL BEARING - ROTOR SYSTEM I - EFFECTS OF MOUNT STIFFNESS AND DAMPING		5. Report Date February 1970 6. Performing Organization Code
7. Author(s) Zolton N. Nemeth and William J. Anderson		8. Performing Organization Report No. E-5273
9. Performing Organization Name and Address Lewis Research Center National Aeronautics and Space Administration Cleveland, Ohio 44135		10. Work Unit No. 129-03 11. Contract or Grant No. 13. Type of Report and Period Covered Technical Note
12. Sponsoring Agency Name and Address National Aeronautics and Space Administration Washington, D. C. 20546		14. Sponsoring Agency Code

15. Supplementary Notes

16. Abstract

The motion of a vertically mounted rotor in a three-pad tilting-pad gas journal bearing was observed for pressurized operation in air. The bearing pads were 2.02 in. (5.1 cm) in diameter and 1.50 in. (3.8 cm) long. The L/D ratio was 0.75. One pad was mounted on a flexible diaphragm. External pressure ranged from 0 to 100 psig (0 to 690 kN/m^2) and speeds to 38 500 rpm for diaphragms of two different stiffnesses with and without damping. The amplitude of rotor motion increased with increasing pressure. The stiffer diaphragm produced smaller amplitudes in general. Diaphragm damping was effective in reducing the amplitude of motion only in the direction normal to the diaphragm.

17. Key Words (Suggested by Author(s)) Bearing Gas bearing Pivoted pad journal bearing	18. Distribution Statement Unclassified - unlimited		
19. Security Classif. (of this report) Unclassified	20. Security Classif. (of this page) Unclassified	21. No. of Pages 26	22. Price* $3.00

*For sale by the Clearinghouse for Federal Scientific and Technical Information
Springfield, Virginia 22151

DYNAMIC BEHAVIOR OF AIR LUBRICATED PIVOTED-PAD JOURNAL BEARING - ROTOR SYSTEM I - EFFECTS OF MOUNT STIFFNESS AND DAMPING

by Zolton N. Nemeth and William J. Anderson

Lewis Research Center

SUMMARY

Experiments were conducted with a vertically mounted rotor supported in two three-pad tilting-pad gas journal bearings with pressurization capability. The bearing pads were 2.02 inches (5.1 cm) in diameter and 1.50 inches (3.8 cm) long. The L/D ratio was 0.75. Each pad was individually pivoted. Two of the pivots were rigidly mounted, and the third pivot was diaphragm flexure mounted. Diaphragms with either 3400 or 22 800 pounds per inch (6×10^5 or 40×10^5 N/m) stiffness were used. The bearings were preloaded at zero speed. No net load was applied to the bearings. The tests were run over a pressure range from 0 to 100 psig (690 kN/m^2) and a speed range of 0 to 38 500 rpm. No external heat was added.

The amplitude of motion at the first two critical speeds increased greatly with increasing supply pressure. The stiffer diaphragm produced smaller amplitudes of motion in general. The motion at the critical speeds was highly elliptical because of the assymmetric stiffness around the bearing produced by two rigidly mounted pivots and the one flexure mounted pivot. Diaphragm damping was effective in reducing the rotor motion at the first critical speed but not at the second critical speed because of the orientation of the elliptical orbit. Damping was effective in reducing the amplitude of motion only in the direction normal to the diaphragm. With the 3400-pound-per-inch (6×10^5-N/m) diaphragm a very small amplitude radial resonance of the diaphragm-mounted pad assembly appeared under pressurized operation at rotor speeds from 31 500 to 34 000 rpm. The frequency of the radial resonance was at twice shaft speed. No other pad resonances or rotor fractional frequency whirl appeared.

INTRODUCTION

Gas bearings in general, including the tilting-pad journal bearing, provide advantages for gas-cycle turbomachinery over conventional oil lubricated bearings, whether fluid film or rolling contact. These advantages are system simplicity, operating capability at high temperatures, and, even in the presence of nuclear radiation, long life.

Powerplant simplicity is attained with gas lubrication because of elimination of auxiliary equipment that would be needed with oil lubrication such as seals, lubricant pumps, separators, adsorbers, coolers, and tanks.

Complex tilting-pad gas journal bearings are used to support the rotating assembly in the Brayton (gas) cycle space turbomachinery (refs. 1 to 4) because they are inherently stable and reliable (ref. 4). The simpler gas bearing types, such as the plain circular bearing, exhibit under light loading a fractional frequency whirl instability at speeds within the operating range of the machines. In a properly designed tilting-pad bearing (ref. 5), however, fractional frequency whirl is either nonexistent or has a threshold well above the operating speed of the machines.

The tilting-pad journal bearing is complex because of the multiplicity of parts which could introduce additional possible motions and problems. The bearing consists of several curved pads each individually pivoted (fig. 1). In the case of the three-pad bearing, two of the pivots are rigidly mounted, and the third pivot is low-spring-rate flexure mounted to lower the critical speed and the bearing loads when passing through the critical speeds and to provide thermal compensation for high-temperature machines. The softer the flexure, the better the thermal compensation. To maintain preload (a condition where the pivot film clearance is less than the machined-in clearance) at design speed

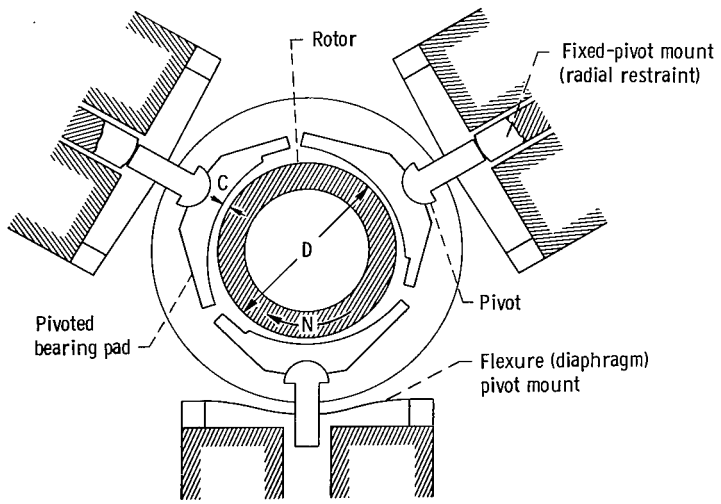

Figure 1. - Tilting pad journal bearing.

which is necessary for stable operation of the pads in pitch, roll, and yaw, the pads have to be highly loaded against the rotor at zero speed. This loading at assembly is sometimes called clamping load. The use of clamping load requires pressurized operation of the bearing from start up to an intermediate speed (approximately 20 000 rpm) where self-acting operation can take over.

Pressurized operation of the bearing further complicates the bearing assembly and necessitates the use of a gas-tight pivot. The pivot can be sealed by a complex pivot assembly containing seals (ref. 6) or by a conforming ball and socket pivot design as is used in the design under investigation (fig. 2).

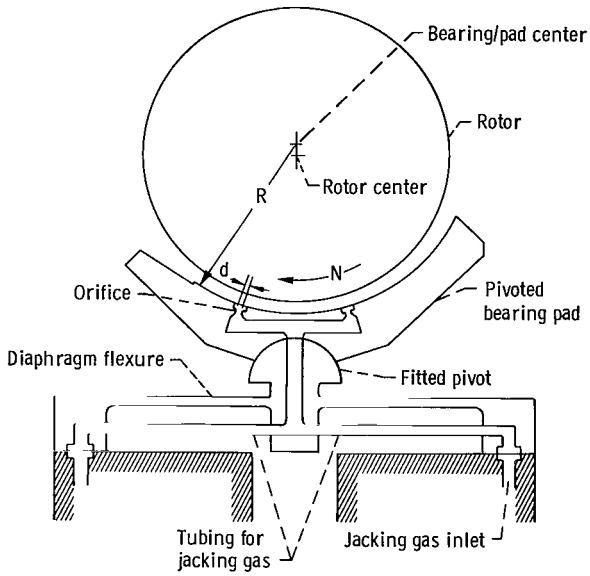

Figure 2. - Flexure mounted journal bearing pad and jacking gas system.

The use of a relatively high stiffness flexure pivot mount might permit startup and operation without a clamping load. Preload of the bearing at design speed would be present. Proper surface coatings would have to be considered to prevent damage to the bearing surfaces from occasional rubs at startup until the pad liftoff speed or self-acting operation is achieved and at shutdown.

Because of the high design speeds of space-power machinery (speeds above 20 000 rpm) the rigid-body critical speeds are traversed both when increasing and decreasing rotor speed. In the critical speed ranges, small exciting forces like residual unbalance in the rotor will produce large amplitudes. It is important that amplitudes of motion be limited in order to avoid unloading the individual pads which would cause them to go into uncontrolled oscillation. Pad-rotor rub and eventual failure could result.

As a result of the complexity of a pivoted-pad bearing incorporating a flexibly

mounted pad, a number of resonances at which motion amplitudes might becomes excessive can occur. The objective of this investigation was, therefore, to determine the effect of flexure (diaphragm) pivot-support stiffness, and damping on pad and rotor-bearing system performance (1) under pressurized operation of 40, 60, 80, and 100 psig (280, 410, 550, and 690 kN/m^2) over the speed range from zero to 38 500 rpm and (2) under self-acting operation from approximately 20 000 rpm to 38 500 rpm.

The bearing size and configuration were similar to those of the bearings in the Brayton cycle turbocompressor (ref. 1) and the Brayton rotating unit. However, the bearings in this investigation were slightly larger, being 2.02 inches (5.1 cm) in diameter and 1.50 inches (3.8 cm) long, whereas the bearings in the Brayton machinery were 1.75 inches (4.4 cm) in diameter. The shoe length-to-diameter ratio L/D was 0.75 in each case. Both bearings had four orifices per pad for the introduction of jacking (external pressurization) gas.

The diaphragm stiffnesses used were 3400 and 22 800 pounds per inch (6×10^5 and 40×10^5 N/m). A low-spring-rate (2000 to 4000 lbf/in. or 3.5×10^5 to 7.0×10^5 N/m) diaphragm was used in the Brayton cycle turbocompressor (ref. 2). Initial clamping forces with the two diaphragms were 12 and 2.3 pounds (53.3 and 10.2 N). The lower clamping force used with the high stiffness diaphragm was just sufficient to load the fitted pivot ball and seat to prevent air leakage during pressurized operation. Higher clamping forces with the stiffer diaphragm would result in excessive preload at high operating speeds.

SYMBOLS

C radial clearance, in.; mm

D bearing (rotor) diameter, in., cm

d orifice diameter, in., cm

F_c clamping load, lbf, N

F_j calibrating force, lbf, N

K diaphragm stiffness, lbf/in., N/m

L bearing length, in., cm

N shaft speed, rpm

R bearing radius, in., cm

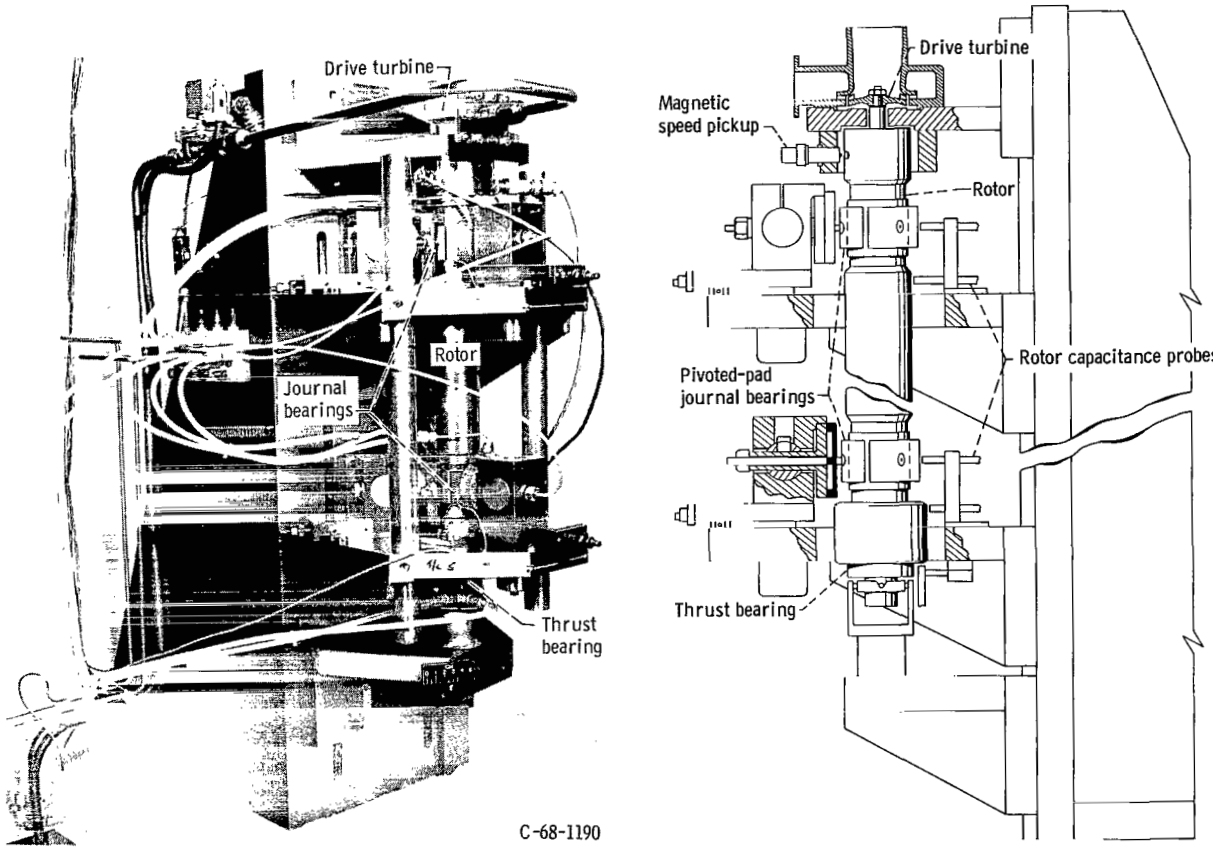

Figure 3. - Pivoted-pad gas journal bearing test apparatus.

APPARATUS

The test rotor is supported vertically by two identical tilting-pad journal bearings spaced 11 inches (28 cm) apart and by an externally pressurized thrust bearing at the lower end. The test apparatus is shown in figure 3. The rotor is driven by an air turbine mounted at the upper end of the rotor. The vertically oriented rotor is used to simulate a gravity free environment on the journal bearings.

Each bearing assembly (pivot flexure and pad) is mounted on an individual support. The supports may be adjusted radially to position the center of the bearing as required. The support brackets may be changed to vary the bearing span.

The rotor is supported at its lower end by an externally pressurized thrust bearing having four 10-mil (254-μm) diameter orifices. The pressure is set at 100 psig (690 kN/m^2), which results in an operating clearance of about 1 mil (25 μm) between the thrust bearing and the rotor. The thrust bearing is mounted on a gimbal support to provide good alinement and tracking with the rotor surface.

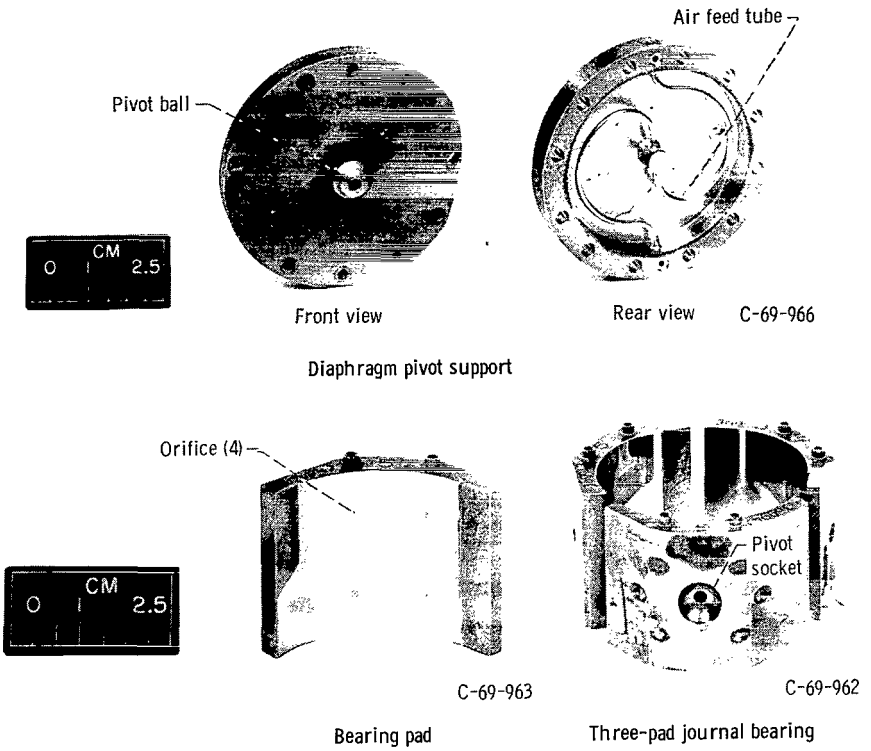

Figure 4. - Tilting-pad journal bearing and diaphragm pivot support.

Test Bearings and Rotor

Pad geometry. - The two journal bearings were self-acting (hydrodynamic) pivoted-pad bearings with provision for pressurized operation. Photographs of the bearing and diaphragm are shown in figure 4. There were three identical pads per bearing. Each had an active arc length of 100^{o}. The pivot was located 65^{o} from the pad leading edge. The pads were about 1.5 inches (3.8 cm) long and had an internal diameter of 2.02 inches (5.1 cm). The L/D ratio was 0.75. The machined diametral clearance between the pad and rotor was 0.0036 inch (91.4 μm). The pressurizing system consisted of four 0.010-inch (254-μm) diameter orifices per pad equally spaced around the pivot away from the maximum pressure generated by self-acting operation (fig. 4). Each orifice ended in a pocket in the pad surface approximately 0.001 inch (25 μm) deep and 0.075 inch (1900 μm) in diameter.

Pivot geometry. - The pivot design was dictated by the necessity to feed pressurized gas through it to the pad surface without leakage. To eliminate complicated pivot seals a conforming ball-socket pivot with a 0.25-inch (0.64-cm) radius was used with a feed hole through the center of pivot assembly (fig. 2).

Diaphragm design. - A flexible mounting configuration for each journal bearing was obtained by mounting one of the pad pivots on a circular thin steel diaphragm or circular

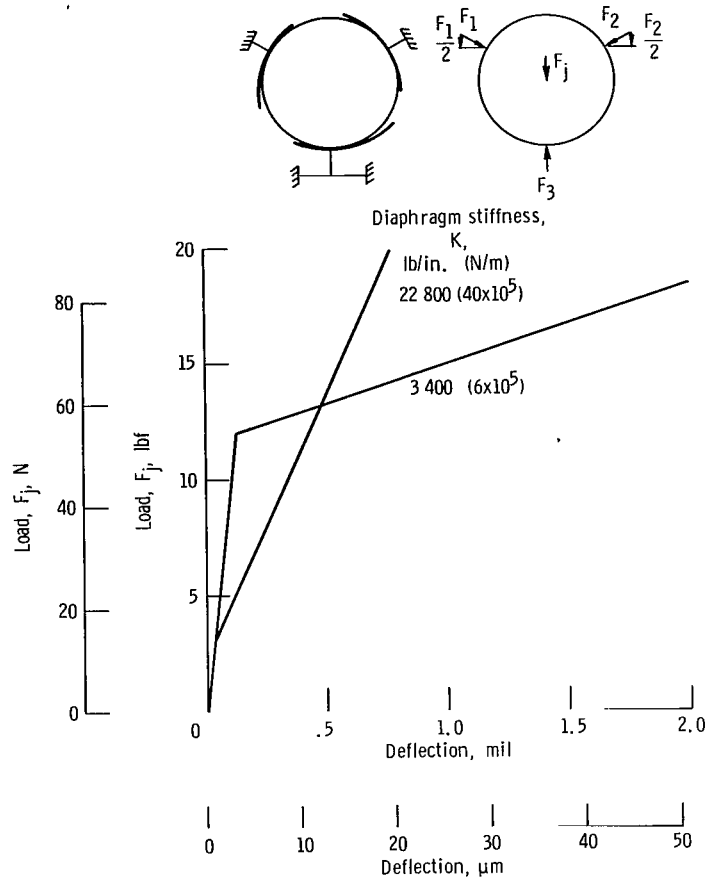

Figure 5. - Measured load versus deflection of two flexure (diaphragm) pivot mounts.

plate (figs. 1 and 2). The remaining two pivots in each bearing were made rigid by stops on diaphragms as shown in figure 1. The stiffness of the diaphragm could be varied by varying its thickness. Two diaphragms were used in these tests. The soft diaphragm had a stiffness of 3400 pounds per inch (6×10^5 N/m) and the stiff diaphragm 22 800 pounds per inch (40×10^5 N/m).

The diaphragms were calibrated as assembled in the test rig with no air pressure to the bearings. The calibrating arrangement is shown schematically in the upper part of figure 5, and the load-deflection curves in the lower part. Initially, before the application of the calibrating force F_j, which is applied to the journal and directed toward the diaphragm, the forces F_1, F_2, and F_3 between the pads and journal are all equal to the clamping load F_c. As the force F_j is increased, the journal deflects in the direction of the diaphragm and the forces F_1 and F_2 decrease. When $F_j = F_c$, $F_1 = F_2 = 0$, and the two rigidly mounted pads become unloaded. When $0 \leq F_j \leq F_c$, the journal moves at a rate governed by the stiffness of the rigidly mounted pads. This corresponds to the high

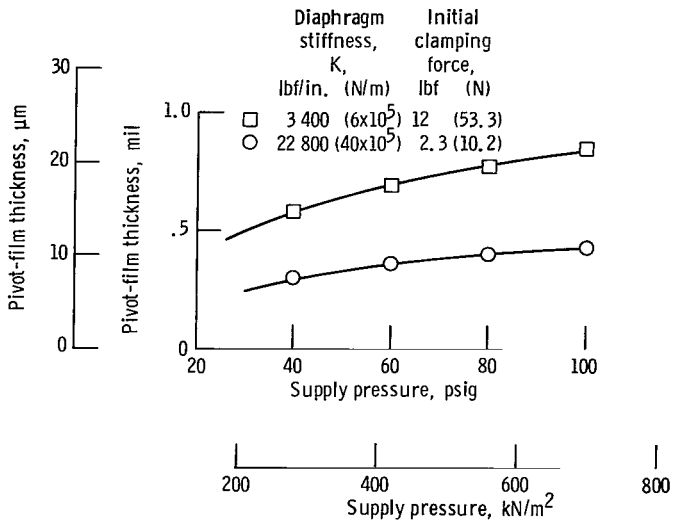

Figure 6. - Variation of pivot film thickness with supply pressure. No rotation.

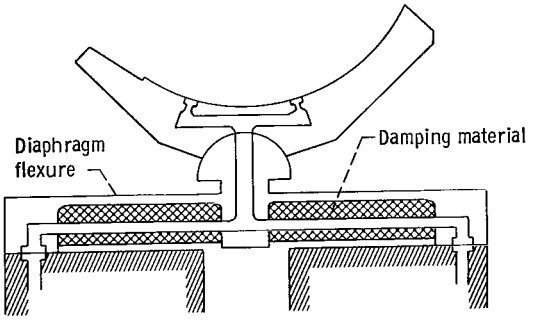

Figure 7. - Journal bearing pad flexure mount damping.

slope portion of each of the load-deflection curves in figure 5. When $F_j \geq F_c$, the diaphragm deflects and the journal moves at a rate governed by the diaphragm stiffness. This corresponds to the lower slope portion of the curves.

The film thickness between the bearing pad and the rotor for pressurized operation differed for the two stiffness diaphragms (see fig. 6). As expected, the film thickness at a given supply pressure was greater for the lower stiffness diaphragm.

The diaphragms were either undamped or damped. Damping was provided in one test for the soft diaphragm (3400 lbf/in. or 6×10^5 N/m stiffness). Damping was accomplished by applying an adherent layer of elastomeric material (18 g) on the underside of the diaphragm (fig. 7).

Air-supply system. - Service air was used for pressurized operation of the test journal bearings and for the thrust bearing and air turbine drive. The air was conditioned to remove moisture, oil vapor, and solid particles before being fed into the bearing. The

pressure of the air was individually regulated to each bearing.

Ambient air in the room was used for self-acting operation of the test journal bearings. The air in the room was kept clean and temperature regulated by a room air conditioner. The temperature was kept constant at 75° F (297 K).

During self-acting operation of the bearings, the jacking gas system was set to come on automatically whenever rotor speed dropped below a preset level. Usually the activating speed was set at about 20 000 rpm.

Rotor geometry. - The test rotor is shown in figure 3. The rotor had mass and inertial properties nominally similar to those of the rotor in the Brayton cycle turbocompressor (ref. 1). The polar and diametral mass moments of inertia of the rotor were 0.035 inch-pound second squared (4.0×10^{-3} kg-m^2) and 1.343 inch-pound second squared (0.152 kg-m^2), respectively (ref. 7). The actual measured weight of the rotor was 16.5 pounds (7.4 kg). The center of gravity was 4.8 inches (12.2 cm) above the centerline of the lower journal. The overall length of the rotor was 20.0 inches (50.8 cm) and bearing span was 11.0 inches (28 cm).

The rotor was of a double overhung design. The turbine and compressor wheel masses and location were simulated by mass concentrations at the ends of the rotor.

The rotor was balanced first in a balancing machine and then in place in the test gas bearings. A check of the balance in place indicated that no final correction was necessary. The center of gravity eccentricity obtained was in the range of 0.0001 inch (2.5 μm) at each journal bearing.

Instrumentation

Capacitance probes. - The displacements and vibrations of the rotor, the bearing pads, and the pad support diaphragm were measured by capacitance probes and vibration meters. Movements as small as 10 microinches could be discerned. The accuracy of the readout instrument was approximately ±3 percent.

Location of the capacitance probes on the rig is shown in figures 3 and 8. There are 15 probes in the rig with seven at each journal bearing and one probe at the end of the rotor to observe its axial motion. The rotor center motion at each journal bearing was monitored by a pair of probes at right angles to each other and designated as X and Y. The X and Y probes were located symmetrically about the axis of the diaphragm flexure mounted pivot. The diaphragm radial motion was monitored by the radial diaphragm probe. A third rotor probe was placed 180° to the diaphragm probe to monitor the relation between the motion of the rotor and the pad flexible diaphragm. The pitch motion of each pad was observed with one probe located on the centerline of each pad and directed toward the center of the bearing.

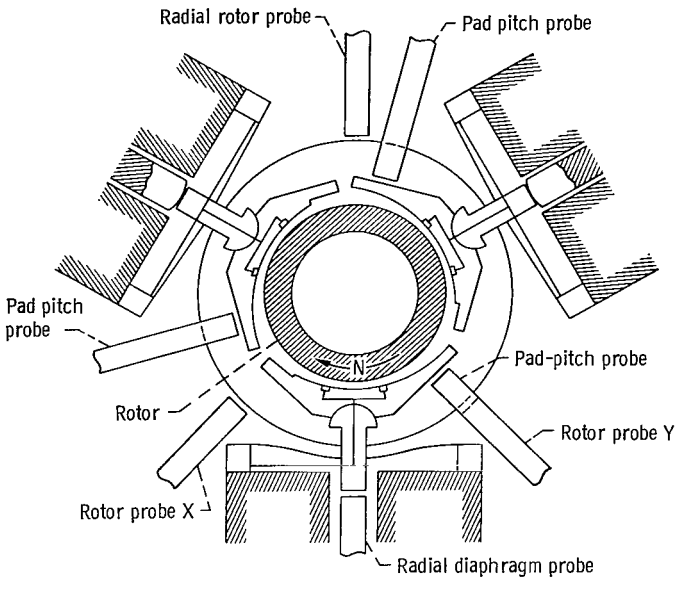

Figure 8. - Capacitance probe location at the bearing and rotor.

The rotor probes at the journal bearings could not be placed at the axial centerline of the bearings because of the interference of the bearing pads. The probes had to be offset about 1.62 inches (4.1 cm) below the center of the bearings. This proved to be inconvenient at times when it was desired to know the location of the rotor center at the journal bearings.

Speed measurement and control. - The speed of rotation of the rotor was measured by means of a magnetic probe. The probe was directed at six shallow drilled holes on the upper diameter of the shaft. The speed could be read directly on an electronic counter. The speed was maintained by an electronic controller to an accuracy of ±1/2 percent. Upper and lower speed limits could be set to limit the maximum speed of the turbine drive and to actuate the jacking gas system at a minimum safe speed, respectively.

Tape system and readouts. - A 14-channel FM tape recorder was used to record the speed of rotation and 12 capacitance-vibration signals. The readout instruments were oscilloscopes, a peak to peak amplitude recorder, and phase angle meters.

Pressure and temperature measurement. - Bearing pad temperatures were measured by iron-constantan thermocouples. The thermocouples were welded on the trailing edge of several of the pads.

Bearing supply pressure and the pressure generated by self-acting operation were measured by Bourdon tube pressure gages (accurate to 0.5 percent).

PROCEDURE

One journal bearing with three pads and one rotor were used for determining the vibrational amplitudes of motion of the rotor-bearing system. Further, the test bearing was always located at the lower bearing position. The upper bearing diaphragm stiffness was kept at a constant 20 600 pound per inch (3.6×10^5 N/m) for all the tests.

The test bearing was first set up with the desired clamping force at zero supply pressure by adjusting the diaphragm flexure assembly in toward the shaft to deflect the diaphragm a measured amount as detected by the capacitance probe. Then the preload value was checked by calibration with weights to obtain a load-deflection curve (fig. 5).

The bearings were then pressurized with air, and the pressure adjusted to the desired value. The temperature of the pressurized air and ambient room air were kept at a constant 75° (297 K) throughout the tests. The speed of the rotor was increased gradually to 38 500 rpm, and, after a few minutes of high-speed operation, the turbine air supply was cut off and the rotor was allowed to coast down in speed to about 2000 rpm. The coastdown lasted approximately 8 minutes. Most of the tests were conducted in the pressurized mode over the entire coastdown speed range. Some coastdown tests were conducted in the self-acting mode to approximately 20 000 rpm and then in the pressurized mode to about 2000 rpm. This procedure was repeated for the various pressures and diaphragms.

The data were continuously recorded on the tape recorder and also observed on oscilloscopes. Detailed observations of the data were made after the test from the tape using the coast down time period.

RESULTS AND DISCUSSION

The results of the experimental investigation are presented in table I and figures 9 to 20. Rotor-bearing dynamic performance of a three-pad pivoted-pad gas journal with one pad flexure mounted is discussed with respect to pressurized and self-acting operation over the speed range to 38 500 rpm. The effects of supply pressure, flexure stiffness, and damping on the amplitude of motion of the rotor were determined, especially at the two rotor critical speeds.

Fractional frequency whirl instability did not, at any time, appear in the course of the experimental investigation. This form of instability is characterized by large amplitude rotor vibrations with vibrational frequency of half, or less, that of the rotor rotational speed. It usually appears in a rotor supported in a full cylindrical fluid film bearing but not a well designed tilting-pad journal bearing.

TABLE I. - ROTOR-BEARING CRITICAL SPEEDS

Diaphragm stiffness, K		Supply pressure, psig (N/m^2)									
		40(280×10^3)		60(410×10^3)		80(550×10^3)		100(690×10^3)		Average	
lb/in.	N/m	Critical speed, rpm									
		1st	2nd	1st	2nd	1st	2nd	1st	2nd	1st	2nd
3 400	6×10^5	7 250	11 200	7 300	11 400	7 200	11 100	7 000	10 800	7 200	11 100
22 800	40	12 800	18 800	12 800	18 700	12 800	18 800	12 750	18 700	12 800	18 800

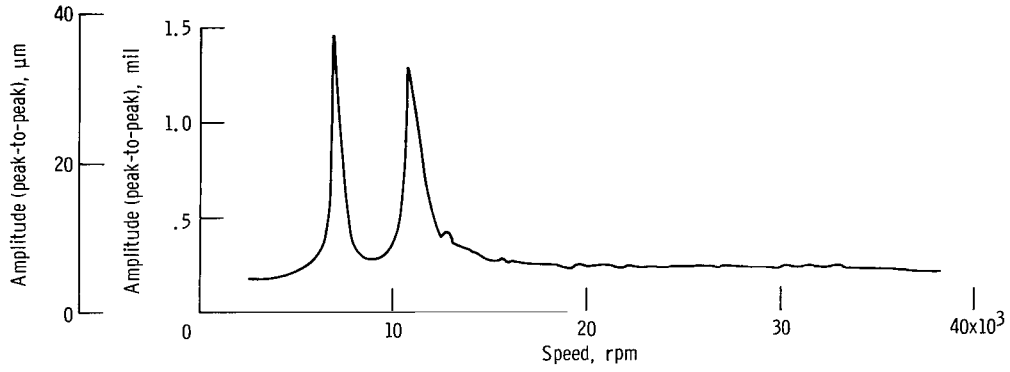

Figure 9. - Rotor response to residual unbalance as detected by rotor probe X. Pressurized operation at 100 psig (690 kN/m^2); diaphragm stiffness, 3400 pounds per inch (6×10^5 N/m).

Pressurized Operation

Critical speeds. - A typical response of the rotor bearing system is shown in figures 9 and 10 over the speed range investigated. This response is at the lower end of the shaft and is caused by synchronous excitation of the residual unbalance of the rotor. The diaphragm flexure stiffness was 3400 pounds per inch (6×10^5 N/m), and the pressure was 100 psig (690 kN/m^2). The first and second critical speeds are traversed as the rotor speed increases and are characterized by large amplitudes of motion. Above these critical speeds the rotor amplitude remains at a constant low value. This amplitude is determined by the distance between the rotor mass center and the geometric center.

The difference in the appearance of the curves at the critical speeds for the same bearing setup can be explained by the nature of the shaft center motion and the placement of the capacitance probes. Figure 11 shows representative oscilloscope traces of the rotor motion at the first two critical speeds. The rotor orbital motion is displayed as well as the rotor motion in the two monitoring planes against the time base. It can be seen that the shaft center motion orbit is highly elliptical at both critical speeds. This

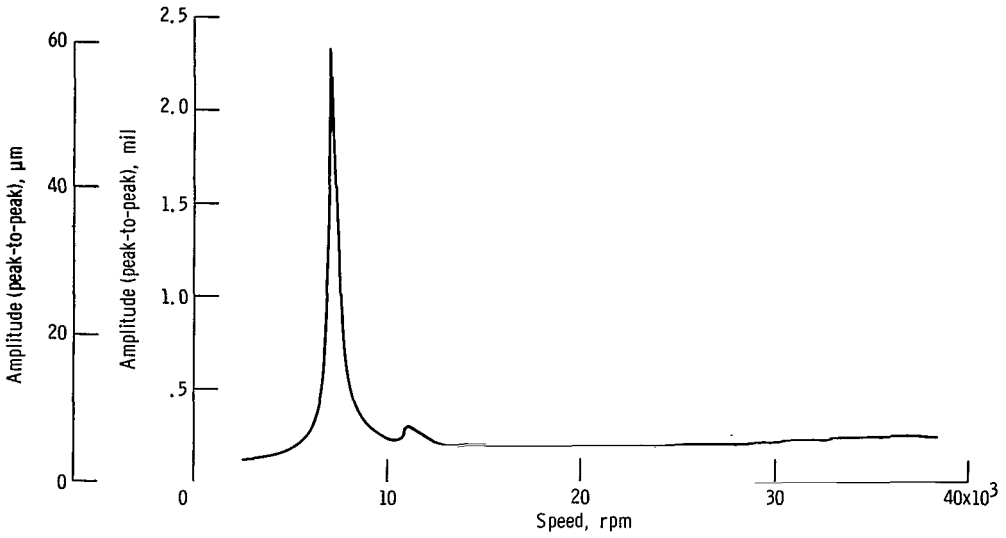

Figure 10. - Rotor response to residual unblance as detected by radial rotor probe. Pressurized operation at 100 psig (690 kN/m^2); diaphragm stiffness, 3400 pounds per inch (6x10^5 N/m).

is due to the fact that stiffness around the bearing is not uniform. The nonuniform stiffness around the bearing is caused by the mounting of two bearing pads on essentially rigid pivots and one bearing pad on a very soft diaphragm mounted pivot.

The orientation of the rotor center orbit is perpendicular to the diaphragm flexure at the first critical speed; thus the X and Y probe motions appear in phase. The rotor moves toward both probes and away from both probes as it oscillates back and forth. The rotor center orbit is parallel to the diaphragm flexure at the second critical speed, and the X and Y probe motions are out of phase by 180^o. The rotor moves toward one probe and away from the other probe at any one time as it oscillates back and forth. The elliptical orbits at the first two critical speeds are approximately perpendicular to each other because of the nonuniform stiffness around the bearing (ref. 5). Both X and Y probes show only a component of the magnitude of amplitude of motion. A probe mounted perpendicular to the diaphragm flexure, such as the radial rotor probe employed in this investigation, would show the true magnitude of the rotor motion at the first critical speed and almost completely miss that at the second critical speed (fig. 10). Proper placement of the motion monitoring probes is important. Possibly, two probes should be used to observe the rotor center movement.

Effect of supply pressure. - Figure 12 shows the effect of supply pressure on the amplitude of rotor motion at the critical speeds. The diaphragm flexure stiffness was 3400 pounds per inch (6×10^5 N/m). The amplitude of motion at both critical speeds increases with increasing supply pressure. It is obvious from these data that the zero load film damping decreases with increasing supply pressure in this type of a bearing system. The amplitude at the first critical speed is greater than at the second critical speed for all values of supply pressure. The response of the rotor with supply pressure is nearly

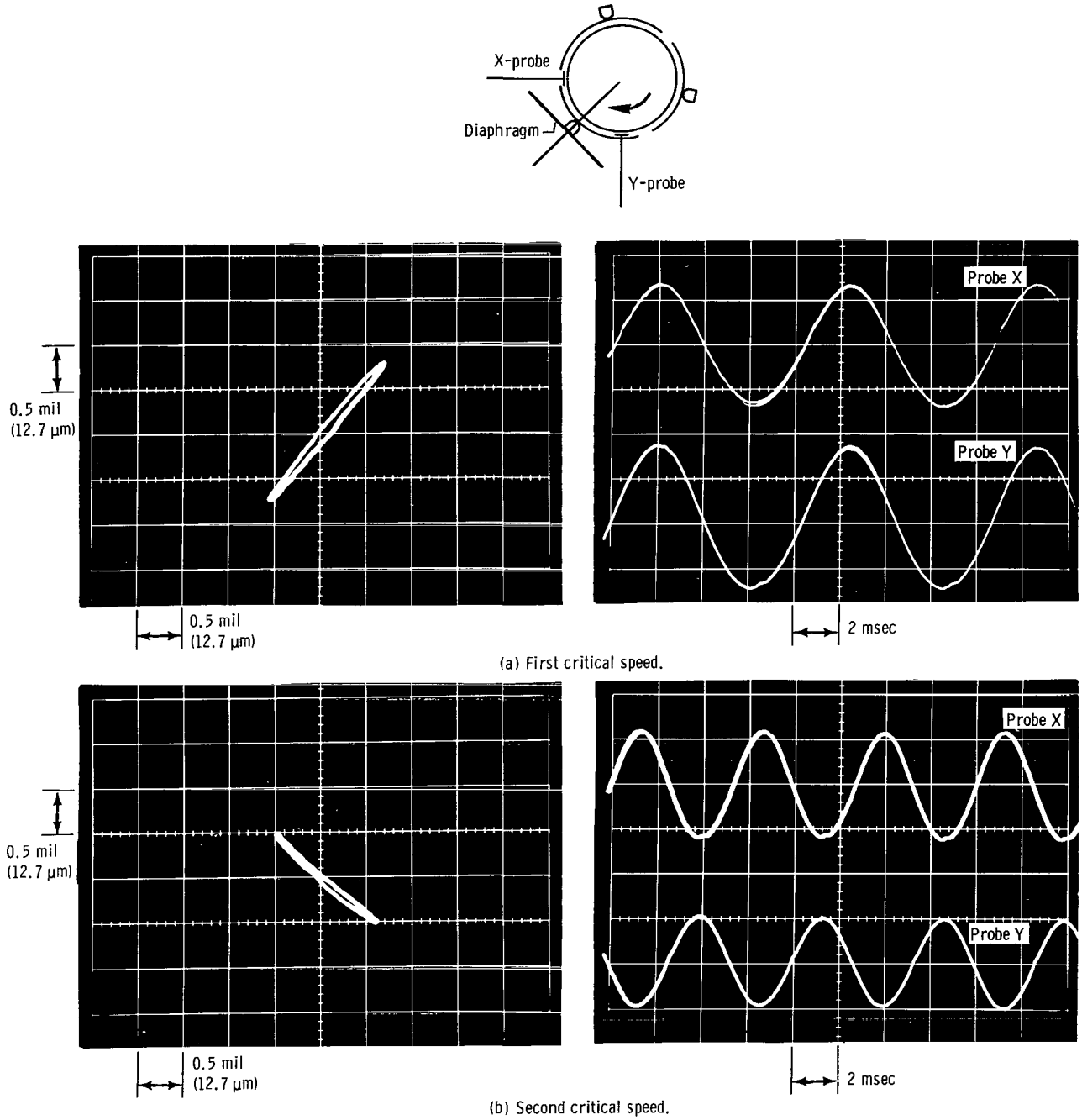

Figure 11. - Motion of rotor with residual unbalance. Supply pressure, 100 psig (690 kN/m^2); diaphragm stiffness, 3400 pounds per inch (6x10^5 N/m).

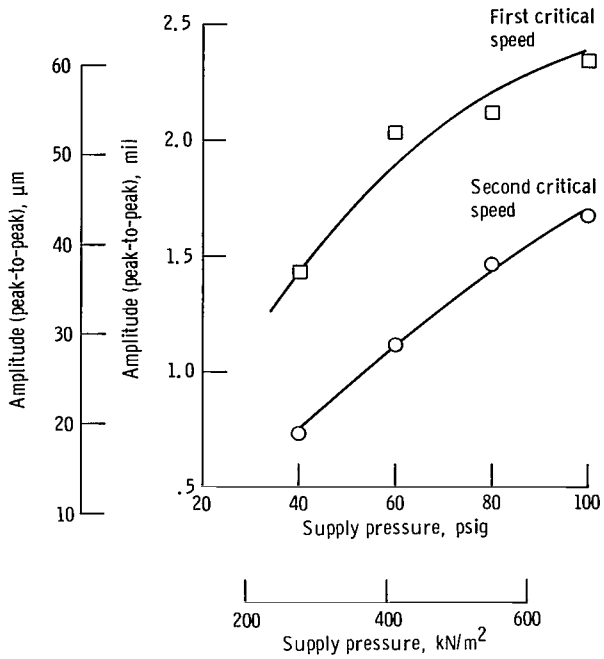

Figure 12. - Rotor response at critical speeds to residual unbalance with supply pressure. Diaphragm stiffness, 3400 pounds per inch (6×10^5 N/m).

linear at the second critical speed, but the response at the first critical speed is not as linear.

The soft diaphragm flexure allows the pad to move radially outward under the rotating load that occurs due to unbalance. This is borne out by the fact that the amplitude of motion is greater than the diametral pivot clearance (fig. 6) for all values of supply pressure.

The motion must be limited because excessively large amplitudes could result in a pad becoming completely unloaded. This in turn could result in pad instability. Several types of pad instability can occur: It can be unstable in pitch, roll, yaw, or, if flexure mounted, the radial direction. For these reasons, it is desirable to limit the amplitude of motion in the critical speeds. One obvious method is to use a supply pressure as low as possible consistent with other system requirements.

Effect of damping. - Another method of reducing the rotor motion at the critical speeds without reducing the film thickness is to introduce damping into the bearing system. The flexure diaphragm was damped as described earlier, and its effect is shown in figure 13 for the first and second critical speeds over the supply pressure range investigated. Figure 13(a) shows that diaphragm damping at the first critical speed is quite effective at all supply pressures. The reduction of rotor amplitude increases with increas-

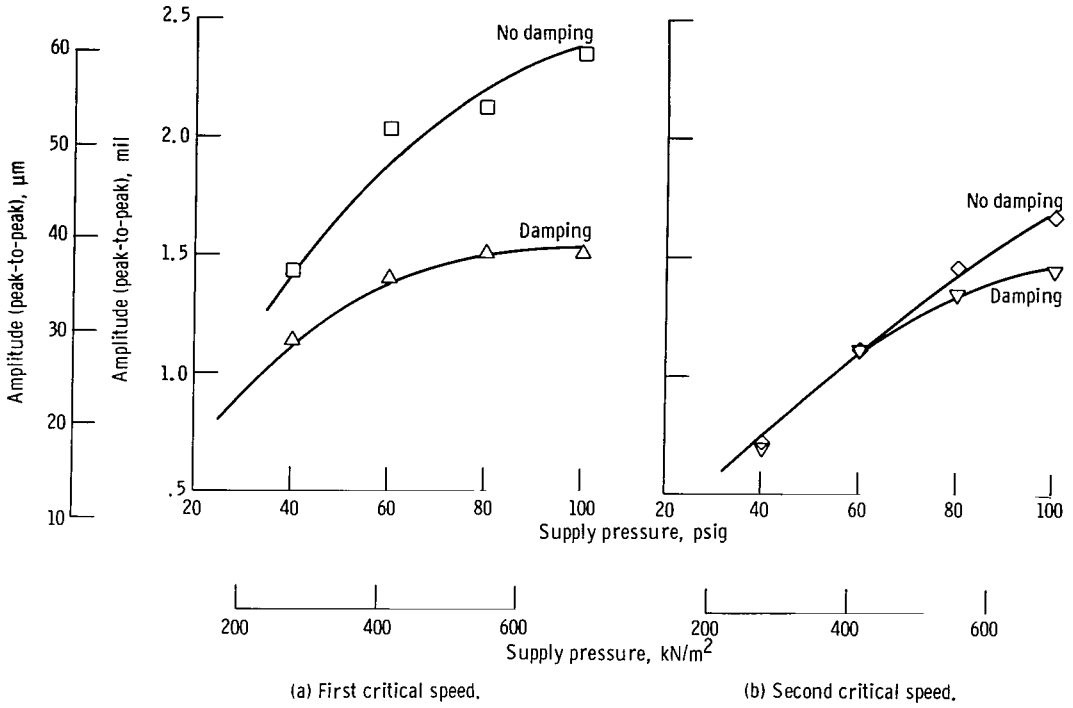

Figure 13. - Rotor response at critical speed to residual unbalance with diaphragm damping with supply pressure. Diaphragm stiffness, 3400 pounds per inch (6×10^5 N/m).

ing supply pressure. Figure 13(b) shows that diaphragm damping at the second critical speed has little effect on the rotor amplitude.

Damping of this type relies on the internal damping in the elastomeric material. Evidently, some minimum amount of motion is required for damping losses to occur as is shown in figure 13(a). Here, at the first critical speed, the diaphragm is actuated perpendicular to its plane causing the damping material to be active. The greater the motion amplitude the greater is the damping effect.

The lack of the damping effect at the second critical speed (fig. 13(b)) is due to the fact that, while the rotor exhibits large amplitudes of motion, the diaphragm does not. The rotor is moving in a highly elliptical orbit parallel to the diaphragm without causing the diaphragm to move radially very much. The damping material does not have an opportunity to damp the motion of the rotor parallel to it.

The presence and amount of damping is usually shown by the characteristic of the phase angle inversion at the first system critical. The phase angle between the amplitude and a mark placed on the rotor changes by 180° as the center of rotor rotation changes from the geometric to the mass center. Figure 14 shows such a phase angle inversion of the rotor at the first critical speed for the damped and undamped diaphragm flexure. Damping causes the rotor inversion to be less steep. The amount of damping is low and is also indicated by the steepness of the curve.

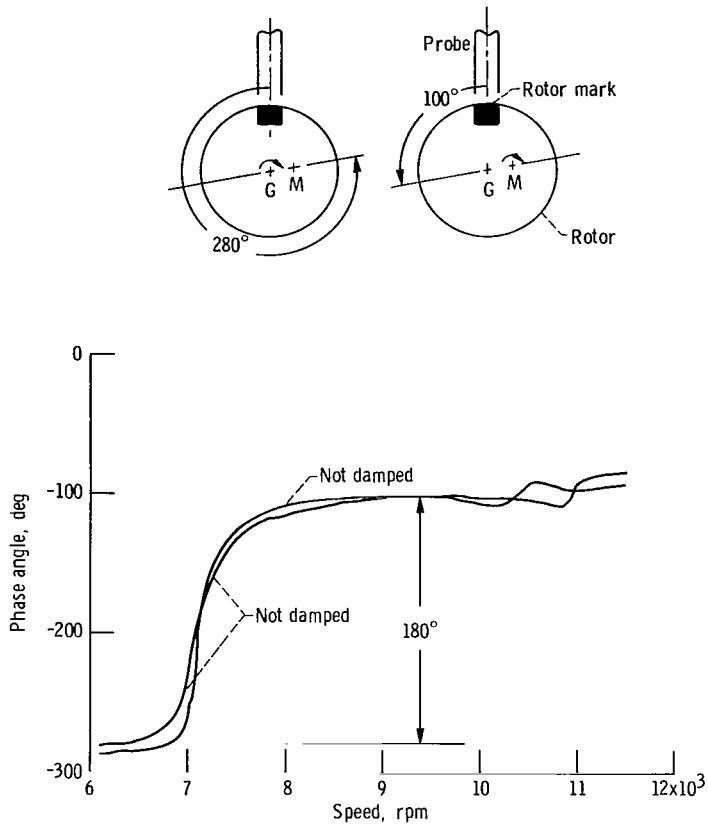

Figure 14. - Phase angle versus speed for damped and undamped diaphragm. Supply pressure, 100 psig (690 kN/m^2); diaphragm stiffness, 3400 pounds per inch (6x10^5 N/m).

Effect of support stiffness. - Still another method of reducing the rotor motion at the critical speeds is to use a higher stiffness diaphragm flexure. The effect of this is shown in figures 15 and 16. A diaphragm flexure stiffness of 22 800 pounds per inch (40×10^5 N/m) was used. The amplitude of rotor motion over the supply pressure range behaved much like that for the lower stiffness diaphragm flexure discussed before; that is, (1) the amplitude of motion at both critical speeds increases with increasing supply pressure, and (2) the amplitude at the first critical speed is greater than at the second critical speed at all values of supply pressure.

Figure 16 shows the effect of diaphragm stiffness on rotor response for two diaphragm stiffnesses of 3400 and 22 800 pounds per inch (6×10^5 and 40×10^5 N/m) over the supply range. Figure 16(a) shows the first critical speed, and figure 16(b) the second critical speed. The motion of the rotor was less with the higher stiffness diaphragm flexure in general at both critical speeds. At the highest pressure of 100 psig (690 kN/m^2) and at the first critical speed, however, the higher stiffness diaphragm gave a slightly greater amplitude than the lower stiffness diaphragm. The difference in ampli-

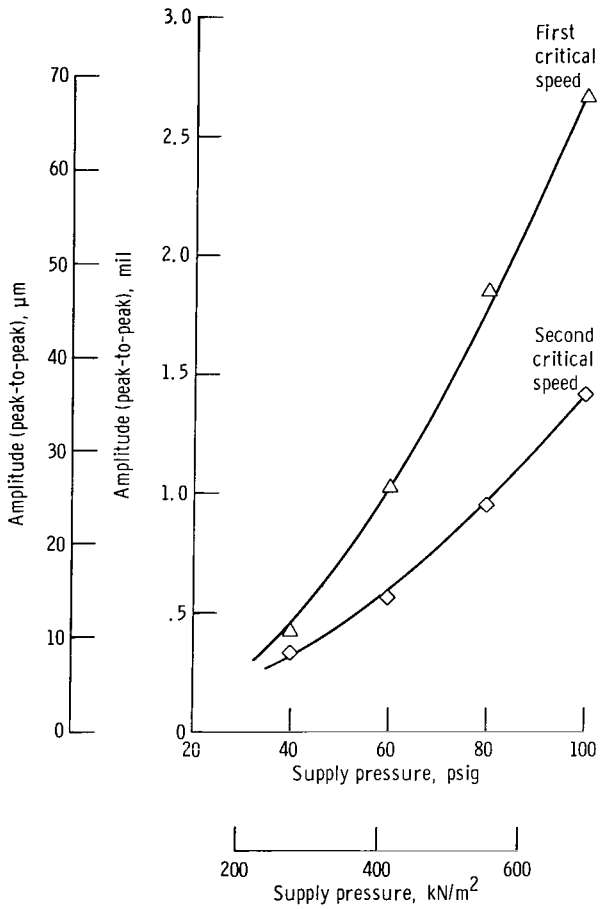

Figure 15. - Rotor response at critical speeds to residual unbalance with supply pressure. Diaphragm stiffness, 22 800 pounds per inch (40×10^5 N/m).

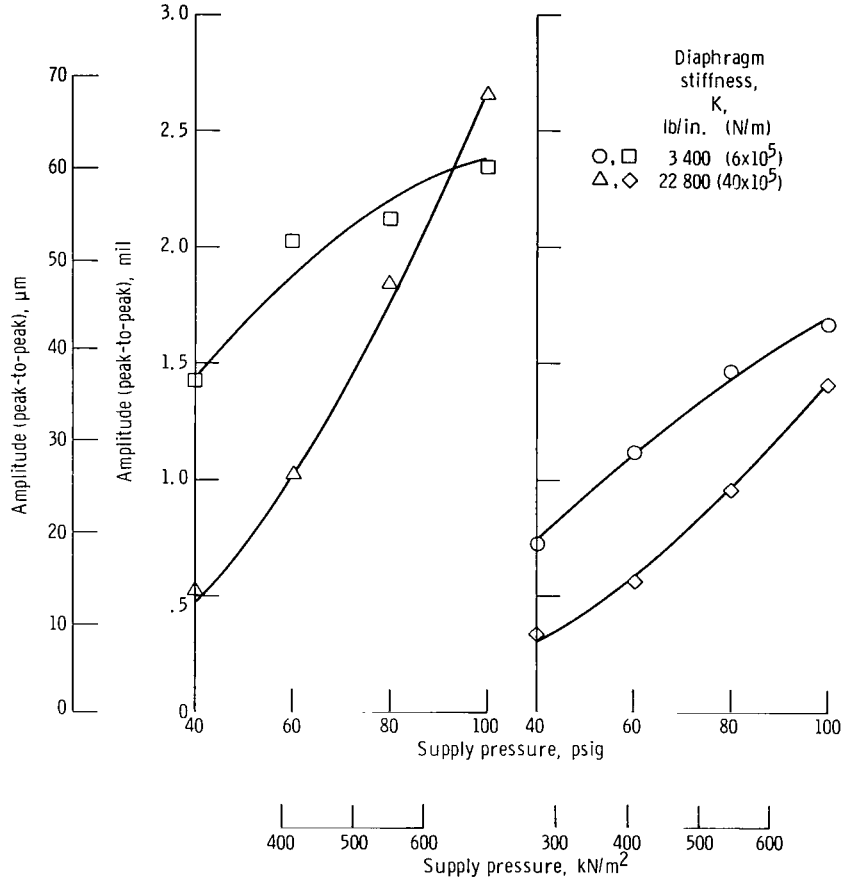

(a) First critical speed. (b) Second critical speed.

Figure 16. - Effect of diaphragm stiffness on rotor response at critical speeds and at various pressures.

tudes of motion for the two diaphragm stiffnesses was approximately constant over the supply pressure range for the second critical speed.

The critical speeds of the system were dependent on the diaphragm flexure stiffness but not on the supply pressure. The average values of the critical speeds were 7200 and 11 100 rpm for the 3400-pound-per-inch (6×10^5-N/m) diaphragm and 12 800 and 18 800 rpm for the 22 800-pound-per-inch (40×10^5-N/m^2) stiffness diaphragm (see table I).

The degree of influence of other variables that change with diaphragm stiffness, such as the location of critical speeds and the film thickness, cannot be assessed at this time.

Effect on component of motion toward the fixed pivots. - At the first critical speed, the major axis of the rotor orbit bisects the separation (120^o) between the two fixed pivots (see fig. 11(a)). The component of motion toward a fixed pivot is then 0.5 times the amplitude of the major axis; that is, as far as the fixed pivot film is concerned, the rotor is moving toward it at 1/2 the actual amplitude.

At the second critical speed, where the rotor orbit is parallel to the diaphragm, the rotor orbit motion component toward a fixed pivot is 0.866 times the amplitude of the major axis. The fixed pivot sees motion toward it which is 0.866 times the actual amplitude.

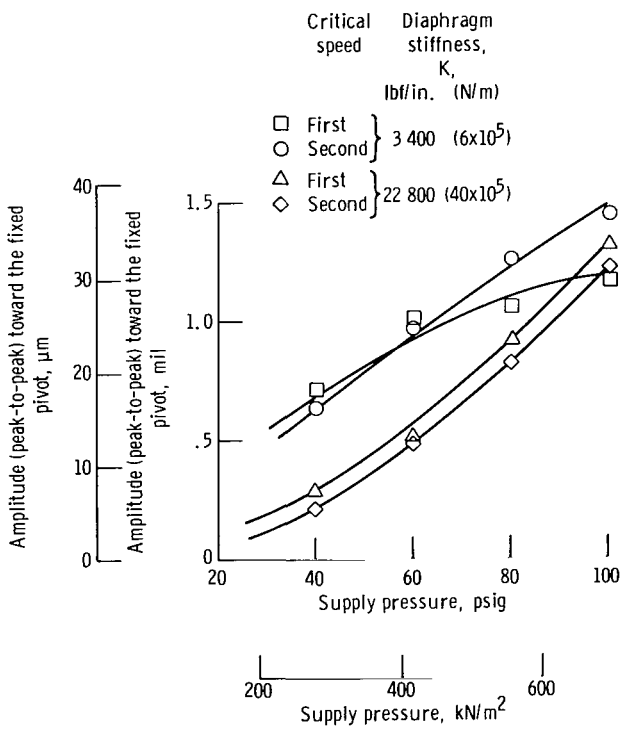

Figure 17. - Component of rotor response toward fixed pivot at critical speeds.

A comparison of the component of rotor motion toward the fixed-pivot at the first and second critical speeds (fig. 17) shows them to be roughly equal over the supply pressure range. This holds for both stiffnesses of diaphragm flexures. This effect probably indicates the presence and operation of film damping (refs. 8 and 9).

Bearing pad resonance. - The diaphragm flexure pivoted-pad assembly exhibited a very small amplitude radial response in the speed range from approximately 31 500 to

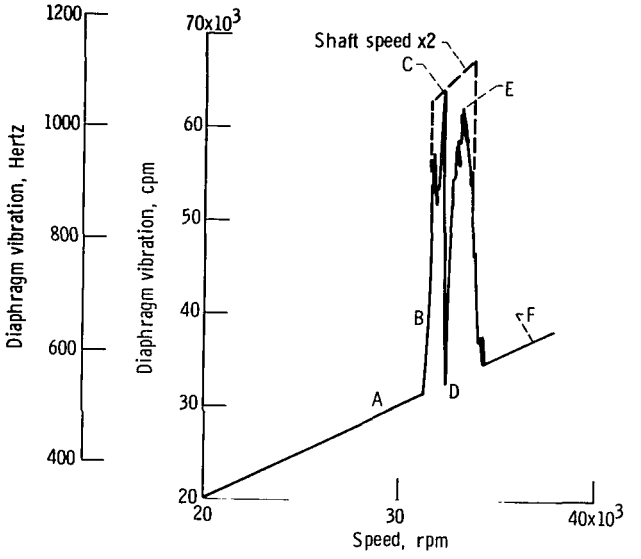

Figure 18. - Diaphragm response with shaft speed. Supply pressure, 100 psig (690 kN/m^2); diaphragm stiffness, 3400 pounds per inch (6×10^5 N/m).

34 000 rpm with the 3400 pound-per-inch (6×10^5-N/m) diaphragm. The frequency of radial response was twice the shaft speed as shown in figure 18. Figure 19 shows six oscillograph views of the shape of the wave form of the radial resonance of the diaphragm pad assembly at various speeds in the resonance range. These waveforms are typical and have been observed in other pivoted-pad bearings. The synchronous frequency measured by the readout instrument at point D (fig. 18) is considered to be spurious because the amplitude of the small waves was not sufficient to actuate the counter.

The diaphragm damping employed in this investigation had no effect on this radial resonance probably because the radial motion is very slight. It was seen that, to be effective, diaphragm motion had to be greater than is present in the radial resonance.

No radial resonance was observed in this speed range when the bearing was in self-acting operation. Possibly the film damping prevented it.

The shaft did not show the influence of the pad diaphragm radial resonance (the twice

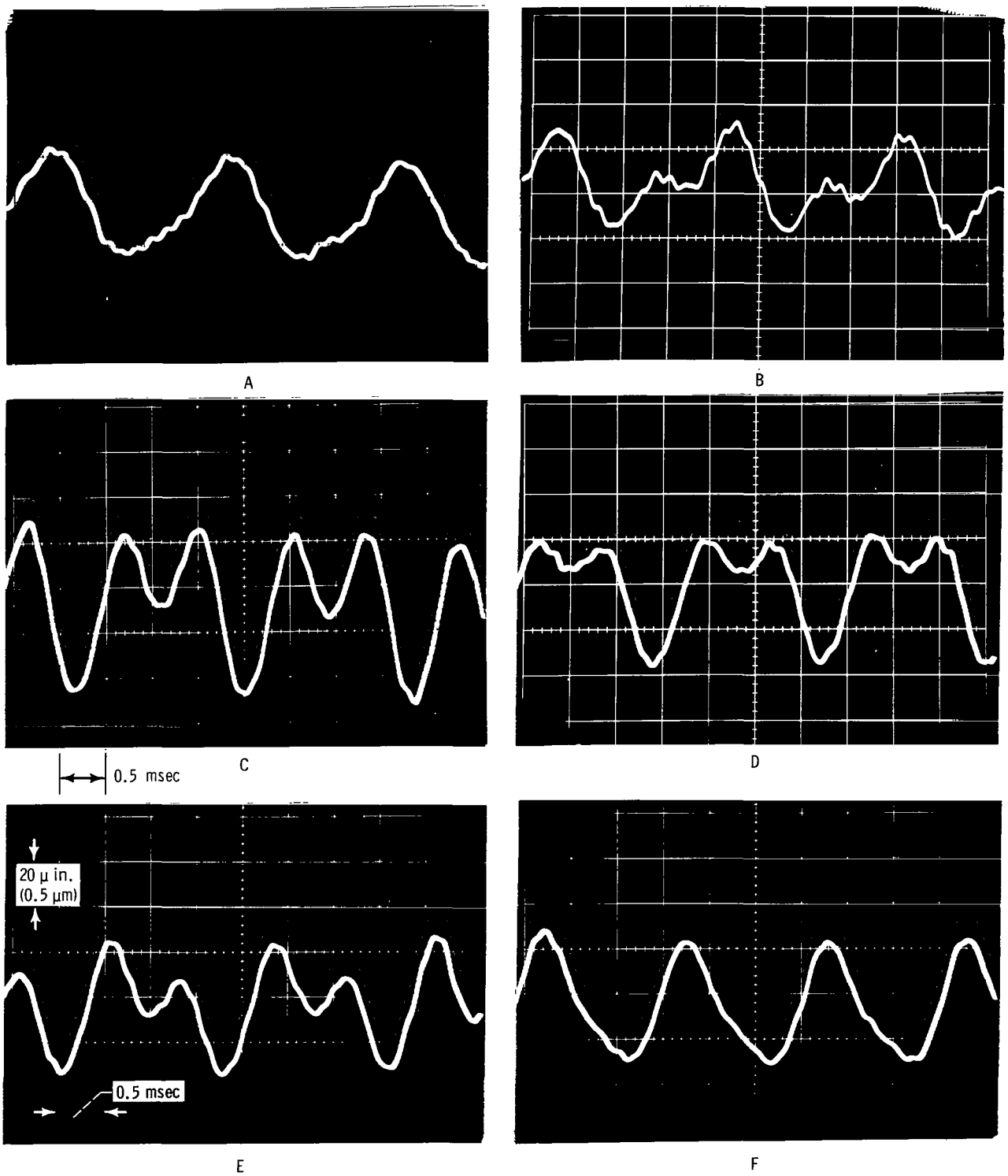

Figure 19. - Oscillographs of radial motion of diaphragm pad assembly at various points shown in figure 18.

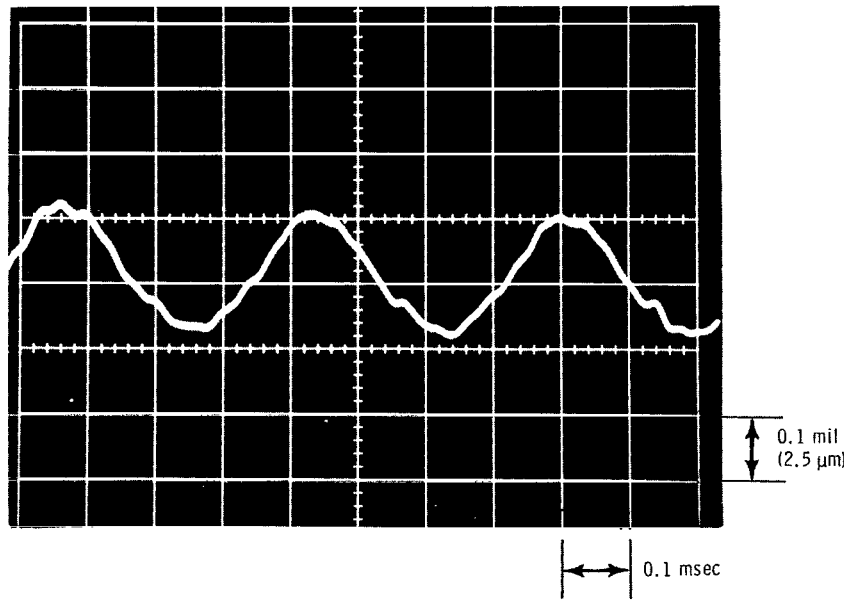

Figure 20. - Shaft response at point C shown in figure 20 as seen by shaft radial probe.

synchronous frequency motion) at point C in figure 19 at 32 200 rpm. This is shown in figure 20 in the shaft response oscillograph view.

Self-Acting Operation

Because of the heavy preload or clamping load, self-acting operation is not possible through the first two critical speeds, but it is feasible in the speed range from 20 000 to 38 500 rpm where sufficient film thickness is generated. Self-acting operation of the pivoted pad bearings was uneventful as no problems occurred. As mentioned above, no radial resonances of the flexure pivoted pad assembly occurred while operating in the self-acting mode.

The bearing pads ran hotter under self-acting conditions than under pressurized operation because of the smaller film thickness and because of less air flow through the bearing space.

SUMMARY OF RESULTS

A series of rotor-bearing dynamic tests was conducted with a vertically oriented rotor mounted in two self-acting three-pad tilting-pad gas journal bearings with four orifices in each pad for pressurized operation. The bearing pads were 2.02 inches

(5.1 cm) in diameter and 1.50 inches (3.8 cm) long. The L/D ratio was 0.75. Each pad was individually pivoted with one pivot in each bearing diaphragm flexure mounted and the other two pivots rigidly mounted. Tests were run in air over a range of external supply pressures from 0 to 100 psig (690 kN/m^2) and a speed range of 0 to 38 500 rpm with diaphragms of two different stiffnesses. The following results were obtained:

1. The amplitude of rotor motion at the first and second critical speeds increased with increasing supply pressure for both stiffness diaphragms of 3400 and 22 800 pounds per inch (6×10^5 and 40×10^5 N/m). The amplitude at the first critical speed was greater than the amplitude at the second.

2. The amplitude of rotor motion was generally less with the 22 800-pound-per-inch (40×10^5-N/m) diaphragm over the range of supply pressures.

3. Externally applied damping of the diaphragm was evaluated with the 3400-pound-per-inch (6×10^5-N/m) diaphragm. It was effective in reducing the amplitude of rotor motion at the first critical speed, but not at the second critical speed. External damping was not effective at the second critical speed because the highly elliptical rotor orbit was oriented parallel to the diaphragm and did not activate the damping material. External damping was most effective with higher supply pressures.

4. The components of rotor motion toward the fixed pivot at the first and second critical speeds were equal, suggesting that film damping was probably present.

5. Variation of gas supply pressure had no effect on the critical speeds.

6. A radial resonance of the diaphragm flexure pivoted-pad assembly at a frequency twice the rotor speed appeared at rotor speeds from approximately 31 500 to 34 000 rpm for the 3400-pound-per-inch (6×10^5-N/m) diaphragm during pressurized operation. It did not appear under self-acting operation. The amplitude of the resonant motion was very small, posing no hazard to bearing operation.

7. The instability commonly called fractional frequency whirl did not appear in the course of the experimental investigation.

Lewis Research Center,
National Aeronautics and Space Administration,
Cleveland, Ohio, November 21, 1969,
129-03.

REFERENCES

1. Anon.: Design and Fabrication of a High-Performance Brayton Cycle Radial-Flow Gas Generator. NASA CR-706, 1967.

2. Wong, R. Y.; Stewart, W. L.; and Rohlik, H. E.: Pivoted-Pad Journal Gas Bearing Performance in Exploratory Operation of Brayton Cycle Turbocompressor. J. Lubr. Tech., vol. 90, no. 4, Oct. 1968, pp. 687-696.

3. Curwen, P. W.; Frost, A.; and Arwas, E. B.: Gas Bearing Systems for NASA Solar Brayton Cycle Axial Flow Turbocompressor and Turboalternator. Presented at ASME Spring Lubrication Symposium, New York, June 9, 1965.

4. Curwen, P. W.; Jones, H. F.; and Schwarz, H.: Application of Gas Bearings to Closed-System Brayton-Cycle Turbomachinery - Recent Accomplishments and Potential Problem Areas. J. Eng. Power, vol. 88, no. 4, Oct. 1966, pp. 367-377.

5. Gunter, E. J., Jr.; Hinkle, J. G.; and Fuller, D. D.: Design Guide for Gas-Lubricated Tilting-Pad Journal and Thrust Bearings with Special Reference to High-Speed Rotors. Rep. I-A2392-3-1, Franklin Inst. Res. Lab. (AEC Rep. NYO-2512-1), Nov. 1964.

6. Frost, A.; Lund, J. W.; and Curwen, P. W.: High-Performance Turboalternator and Associated Hardware. 2: Design of Gas Bearings. NASA CR-1291, 1969.

7. Anon.: Investigations of Gas Bearing Compressibility Number and Pivot Flexure in Tilting Pad Bearings. Rep. APS-5223-R, AiResearch Mfg. Co. (NASA CR-54939), Mar. 31, 1967.

8. Hunt, J. B.: How Lubricant Film Affects Dynamic Response of Machines. The Engineer, vol. 226, no. 5888, Nov. 29, 1968, pp. 831-834.

9. Lund, J. W.: Calculation of Stiffness and Damping Properties of Gas Bearings. J. Lubr. Tech., vol. 90, no. 4, Oct. 1968, pp. 793-803.

NASA-Langley, 1970 — 15 E-5273

"The aeronautical and space activities of the United States shall be conducted so as to contribute . . . to the expansion of human knowledge of phenomena in the atmosphere and space. The Administration shall provide for the widest practicable and appropriate dissemination of information concerning its activities and the results thereof."

—NATIONAL AERONAUTICS AND SPACE ACT OF 1958

NASA SCIENTIFIC AND TECHNICAL PUBLICATIONS

TECHNICAL REPORTS: Scientific and technical information considered important, complete, and a lasting contribution to existing knowledge.

TECHNICAL NOTES: Information less broad in scope but nevertheless of importance as a contribution to existing knowledge.

TECHNICAL MEMORANDUMS: Information receiving limited distribution because of preliminary data, security classification, or other reasons.

CONTRACTOR REPORTS: Scientific and technical information generated under a NASA contract or grant and considered an important contribution to existing knowledge.

TECHNICAL TRANSLATIONS: Information published in a foreign language considered to merit NASA distribution in English.

SPECIAL PUBLICATIONS: Information derived from or of value to NASA activities. Publications include conference proceedings, monographs, data compilations, handbooks, sourcebooks, and special bibliographies.

TECHNOLOGY UTILIZATION PUBLICATIONS: Information on technology used by NASA that may be of particular interest in commercial and other non-aerospace applications. Publications include Tech Briefs, Technology Utilization Reports and Notes, and Technology Surveys.

Details on the availability of these publications may be obtained from:

SCIENTIFIC AND TECHNICAL INFORMATION DIVISION

NATIONAL AERONAUTICS AND SPACE ADMINISTRATION

Washington, D.C. 20546